

# DP-SGD for non-decomposable objective functions

William Kong      Andrés Muñoz Medina      Mónica Ribero \*

October 6, 2023

## Abstract

Unsupervised pre-training is a common step in developing computer vision models and large language models. In this setting, the absence of labels requires the use of similarity-based loss functions, such as contrastive loss, that favor minimizing the distance between similar inputs and maximizing the distance between distinct inputs. As privacy concerns mount, training these models using differential privacy has become more important. However, due to how inputs are generated for these losses, one of their undesirable properties is that their  $L_2$  sensitivity can grow with increasing batch size. This property is particularly disadvantageous for differentially private training methods, such as DP-SGD. To overcome this issue, we develop a new DP-SGD variant for similarity based loss functions — in particular the commonly used contrastive loss — that manipulates gradients of the objective function in a novel way to obtain a sensitivity of the summed gradient that is  $O(1)$  for batch size  $n$ . We test our DP-SGD variant on some preliminary CIFAR-10 pre-training and CIFAR-100 finetuning tasks and show that, in both tasks, our method’s performance comes close to that of a non-private model and generally outperforms DP-SGD applied directly to the contrastive loss.

## 1 Introduction

Foundational models — large models trained in an unsupervised manner to be fine-tuned on specific tasks— have become one of the cornerstones of modern machine learning. These models have generally outperformed other approaches in multiple tasks, ranging from language generation, to image classification and speech recognition. In fact, models such as LaMDA [36], BERT [10], GPT [29] and diffusion models [32, 1] are now at the frontier of the generative AI revolution and are interacting with millions of users per day. Due to the complexity of these models, there are multiple concerns in the privacy community that these models may *memorize* some of the training data. For models trained on

---

\*Google Research NYC. {weiweikong, ammedina, mribero}@google.com

user-generated content, this may result in a catastrophic privacy breach, where the model may unintentionally reveal private information about a user. Recent work from [34, 3] has shown that these risks are not just a theoretical concern and that it is possible to (i) know whether a particular example was in a dataset for training the model and (ii) reconstruct training data using only black box access to the model. On the other hand, the same line of research has shown that these attacks become significantly harder when models are trained using differential privacy. This is generally expected as differential privacy provides an information theoretic guarantee that the model does not depend drastically on any example.

It is for the above reason that private training methods have received considerable attention from the privacy community in the past decade. Some of the foundational work on this area was set by [6] who provided algorithms for private learning with convex loss functions and [2] who proposed the now celebrated differentially private stochastic gradient descent (DP-SGD) algorithm for training neural networks in a private way. Multiple lines of work have stemmed from this research area, ranging from tighter privacy analysis [13] to more efficient implementations of DP-SGD [23]. However, most of the literature on private machine learning makes one crucial assumption about the objective function they are trying to minimize: the objective decomposes as a sum (or average) of example level losses. This assumption drastically simplifies the *sensitivity analysis* (how the objective changes as one changes one point in the dataset) of DP-SGD algorithm.

In this work, we focus on models that are trained using non-decomposable objectives. That is, an objective function that cannot be described as a sum (or average) of individual losses. Our study is motivated by the use of contrastive losses [7, 8] for pre-training foundational models. Contrastive losses generally compare each example against all other examples in the batch. That is, adding or removing an example to a batch of examples can affect the objective function in unpredictable ways. This type of behavior generally makes it hard, if not impossible, to train models privately. In this work however, we show that common non-decomposable losses have a critical property that makes them amenable to private training. Our contributions are summarized as follows:

- We provide a general framework for measuring the sensitivity of DP-SGD with non-decomposable objectives.
- We show how to apply this framework to two non-decomposable losses: contrastive loss and the spreadout (regularization) loss [43].
- We conduct experiments on privately pre-training image classification models and show that we can achieve performance comparable to non-private pre-training. Our experiments analyze the performance of simple pre-training as well as fine tuning on a downstream task.

## 2 Preliminaries and Notation

Given a non-Euclidian feature space  $\mathcal{X}$ , such as a space of images or sentences, we focus on unsupervised learning of embedding models  $\Phi_w : \mathcal{X} \rightarrow \mathbb{R}^d$  parametrized by  $w \in \mathcal{W}$  where  $\mathcal{W}$  is a parameter space  $\mathcal{W} \subset \mathbb{R}^p$ .

Let  $\mathcal{D} = \{(x_i, x'_i)\}_{i=1}^n \subseteq \mathcal{X} \times \mathcal{X}$  be a batch with  $n$  records, such that  $x_i$  and  $x'_i$  are similar (positive pairs) in the feature space. These positive pairs can correspond, for instance, to two version of the same image, a sentence and its translation on a different language or an image and its caption. Let  $S : \mathbb{R}^d \times \mathbb{R}^d \rightarrow \mathbb{R}$  be a function measuring similarity of two points in  $\mathbb{R}^d$ , the objective is to find a parameter  $w \in \mathcal{W}$  that preserves the similarities defined by pairs in  $\mathcal{D}$ .

Given vectors  $x_1, \dots, x_n \in \mathbb{R}^d$ , define  $\mathbf{x} = (x_1, \dots, x_n)$ , and denote  $\Phi(\mathbf{x}) = (\Phi(x_1), \dots, \Phi(x_n))$ . Given embeddings  $u, v_1, v_2, \dots, v_m \in \mathbb{R}^d$ , define the similarity profile of  $u$  respect to  $v_1, \dots, v_m$  for  $m \leq n$  as the vector  $\mathbf{S}^m(u, \mathbf{v})$  of similarities between  $u$  and the first  $m$  vectors in  $\mathbf{v}$ . Formally,  $\mathbf{S}^m(u, \mathbf{v}) \in \mathbb{R}^m$  where entry  $j$  for  $j = 1, \dots, m$  is defined as  $[\mathbf{S}^m(u, \mathbf{v})]_j = S(u, v_j)$ .

Given a batch  $X = \{(x_1, x'_1), \dots, (x_n, x'_n)\}$  and a family of loss functions  $\ell^{(i,n)} : \mathbb{R}^n \rightarrow \mathbb{R}$  that calculate the loss on the similarity profile of point  $x_i$  based on the  $n$  points on batch  $X$ , define

$$\mathcal{L}(w, X) = \sum_{i=1}^n \ell^{(i,n)}(\mathbf{S}^n(\Phi_w(x_i), \Phi_w(x'_1), \dots, \Phi_w(x'_n))) \quad (1)$$

Given  $\eta > 0$ , contrastive loss models, which aim to minimize  $\mathcal{L}(\cdot, X)$ , are typically trained iteratively using stochastic gradient descent (SGD) as follows:

$$w_+ = w - \eta(\nabla_w \mathcal{L}(w, X))$$

**Example 1** (Contrastive loss). *Let us provide a more concrete example of the type of losses we are considering. Let  $\phi_w$  denote an embedding function and let*

$$u_{ij} := S(\phi_w(x_i), \phi_w(x'_j)) = \left\langle \frac{\phi_w(x_i)}{\|\phi_w(x_i)\|}, \frac{\phi_w(x'_j)}{\|\phi_w(x'_j)\|} \right\rangle$$

*denote the cosine similarity between the embeddings. The contrastive loss  $\ell^{(i,n)}$  is given by:*

$$\ell^{(i,n)}(u_{i1}, \dots, u_{in}) = -\log \left( \frac{e^{u_{ii}}}{\sum_{j=1}^n e^{u_{ij}}} \right) = \log \left( \sum_{j=1}^n e^{u_{ij}} \right) - u_{ii}$$

*This loss essentially treats the unsupervised learning problem as a classification problem with  $n$  classes, where the pair  $(x_i, x'_i)$  has a positive label and  $(x_i, x'_j)$  has a negative label for all  $j \neq i$ . For this reason we refer to the similarity terms  $u_{ij}$  the contrastive logits.*

The contrastive loss is widely used by the vision community [7, 8, 28] and has been shown to be extremely successful at obtaining pre-trained models for image classification.

**Example 2** (Spreadout regularizer loss). *Let  $u_{ij}$  be defined as in Example 1. The spreadout (regularizer) loss is defined as*

$$\ell^{(i,n)}(u_{i1}, \dots, u_{in}) = \frac{1}{n-1} \sum_{j \neq i} u_{ij}^2$$

The spreadout regularizer is commonly used when training embeddings for computer vision [43, 42] used as a method to promote orthogonality in the embedding space among dissimilar objects and use of the whole feature space.

**Differential Privacy.** Let us now define the notion of differential privacy [11]. Let  $\mathcal{Z}$  denote an arbitrary space and let  $D = \{z_1, \dots, z_n\} \subset \mathcal{Z}$  denote a dataset. We say that datasets  $D$  and  $D'$  are neighbors if  $D' = D \cup \{z_{n+1}\}$  for some  $z_{n+1} \in \mathcal{Z}$ . A mechanism  $M: \mathcal{Z}^* \rightarrow \mathcal{O}$  is a randomized function mapping a dataset to some arbitrary output space. Let  $\epsilon, \delta > 0$ . We say that mechanism  $M$  is  $(\epsilon, \delta)$ -differentially private if for all neighboring datasets  $D, D'$  and all  $S \subset \mathcal{O}$  the following inequality holds:

$$P(M(D) \in S) \leq e^\epsilon P(M(D') \in S) + \delta$$

A simple way of ensuring that a mechanism is differentially private is by using the Gaussian Mechanism.

**Example 3** (The Gaussian Mechanism). *Let  $\epsilon, \delta > 0$  and let  $f: \mathcal{Z}^* \rightarrow \mathbb{R}^d$ . Let  $\Delta = \|f(D) - f(D')\|_2$  denote the  $L_2$ -sensitivity of the function  $f$ . The mechanism defined by*

$$M(D) = f(D) + \Delta \xi,$$

where  $\xi \sim \mathcal{N}(0, \sigma)$ , is  $(\epsilon, \delta)$ -differentially private for an appropriate choice of  $\sigma$  (for example, see [4] for some conditions on  $\sigma$ ).

For the rest of the paper, our goal will be to implement the Gaussian mechanism for the function

$$X \mapsto \nabla_w \mathcal{L}(w, X).$$

**Example 4** (Naive DP-SGD similarity-based loss functions.). *Let  $X = \{(x_1, y_1), \dots, (x_n, y_n)\}$  be a dataset of features and label pairs, and consider a loss function  $\mathcal{L}_{sum}(w, X) = \sum_{i=1}^n f^i(w)$  where  $f^i$  is the example-level loss on example  $(x_i, y_i)$ . DP-SGD implements the gaussian mechanism to privately estimate  $\nabla_w \mathcal{L}_{sum}(w, X)$ , the gradient of  $\mathcal{L}_{sum}(w, X)$  respect to  $w$  given by*

$$\nabla_w \mathcal{L}_{sum}(w, X) = \sum_{i=1}^n \nabla_w f^i(w).$$

The norms of  $\nabla_w \mathcal{L}_{sum}(w, X)$  and individual gradients  $\nabla_w f^i(w)$  are unknown in most settings therefore practitioners select a clip value  $B$  to bound the norm of individual gradients  $\nabla_w f^i(w)$  to the gradient. Estimating an optimal clip norm  $B$  is hard in deep learning settings [20, 33] because small clip values can introduce bias and slow-down (or ruin) convergence [26, 19], while large clip values will result on large amounts of noise being added to the gradient. Adding or removing one example from  $X$  will not change the norm of  $\nabla_w \mathcal{L}_{sum}$  by more than  $B$ , but notice that the batch-gradient  $\nabla_w \mathcal{L}_{sum}(w, X)$  can have norm  $nB$ , mitigating the bias introduced by clipping while the noise magnitude remains constant in  $n$ .

Now consider a dataset  $X = \{(x_1, x'_1), \dots, (x_n, x'_n)\}$  and the loss function  $\mathcal{L}$  defined in eq. (1), which will be denoted  $\mathcal{L}_{sim}(w, X)$  in this example. The gradient  $\nabla_w \mathcal{L}_{sum}$  is given by

$$\nabla_w \mathcal{L}_{sim}(w, X) = \sum_{i=1}^n \nabla \ell^{(i,n)}(\mathbf{S}^n(\Phi_w(x_i), \Phi_w(x'_1), \dots, \Phi_w(x'_n)))$$

Let  $X' = \{(x_1, x'_1), \dots, (x_{n-1}, x'_{n-1})\}$  be a neighboring dataset of  $X$ , and  $\nabla_w \mathcal{L}_{sim}(w, X')$  the gradient computed on  $X'$ .

The sensitivity of  $\nabla_w \mathcal{L}_{sim}$  on  $X$  and  $X'$  is given by

$$\begin{aligned} \|\nabla_w \mathcal{L}_{sim}(w, X) - \nabla_w \mathcal{L}_{sim}(w, X')\| = & \\ & \left\| \nabla \ell^{(n,n)}(\mathbf{S}^n(\Phi_w(x_n), \Phi_w(x'_1), \dots, \Phi_w(x'_n))) \right. + \\ & \sum_{i=1}^n \nabla \ell^{(i,n)}(\mathbf{S}^n(\Phi_w(x_i), \Phi_w(x'_1), \dots, \Phi_w(x'_n))) \\ & \left. - \nabla \ell^{(i,n-1)}(\mathbf{S}^{n-1}(\Phi_w(x_i), \Phi_w(x'_1), \dots, \Phi_w(x'_{n-1}))) \right\| \end{aligned}$$

None of the terms above cancels because  $x'_n$  appears in all the summands. Using triangle inequality it is possible to show that individual terms

$$\begin{aligned} & \nabla \ell^{(i,n-1)}(\mathbf{S}^{n-1}(\Phi_w(x_i), \Phi_w(x'_1), \dots, \Phi_w(x'_{n-1}))) \\ & - \nabla \ell^{(i,n-1)}(\mathbf{S}^{n-1}(\Phi_w(x_i), \Phi_w(x'_1), \dots, \Phi_w(x'_{n-1}))) \end{aligned}$$

are bounded by  $2B$  and the overall sensitivity is bounded by  $2Bn$ . In this case, even with per-example clipping the noise magnitude grows with  $n$ .

Alternatively, clipping directly  $\nabla_w \mathcal{L}_{sim}(w, X)$  to have norm at most  $B$  could reduce the amount of noise added; this is the strategy suggested by [17, 18] which we call Naive-DP in our experiments' section.

### 3 Related work

Contrastive learning has had large impact on unsupervised pretraining of computer vision models [7, 8] and representation learning for language models [25, 9],

or both [28]. [12, 14, 38] use a contrastive loss function for pre-training and fine-tuning BERT with data augmentation. More recently it has been used for reinforcement learning with BERT-type models [5].

In the private setting, the majority of the work has been focused on improving the original implementation of DP-SGD [2] for decomposable losses. Research has particularly focused on tighter privacy guarantees on DP-SGD via advanced privacy accounting methods [27, 13] or solving computational issues associated with gradient clipping [15]. For non decomposable losses, some work has studied private learning from pairwise losses in the convex and strongly convex case ([17, 40]) and test only in the diabetes dataset. Later work [41, 18] obtains similar results for the non-convex case; all these approaches circumvent clipping by assuming access to the Lipschitz constant of the loss function, which depends on the encoder function (typically a deep neural network). However, this Lipschitz constant is generally not easy to estimate and this is an active area of research [20, 33].

In [39] the authors learn private image embeddings with user-level differential privacy, but avoid unsupervised training (and consequently non-decomposable loss functions used for unsupervised pre-training like the contrastive loss, or the triplet loss). Instead, this work relays a supervised multi-class classification problem, and avoids dependencies among different records, at the cost of labeling the data.

In [22] the authors propose noising the similarity matrix between pairs of inputs and compute a noisy loss function. They combine this with a noisy gradient but assume a per-gradient bounded sensitivity.

Orthogonal work study attacks to embedding models. For instance [35] showed that when trained without differential privacy, embedding models can be inverted. More specifically, model attacks designed to recover information from embeddings trained with a contrastive loss are able to recover members from the training set [24]. To prevent specific attacks [30] developed an architecture that learns an obfuscator that prevents reconstruction or attribute inference attacks. [16] quantifies the exposure risk under contrastive learning losses and develops an adversarial training procedure to mitigate the risk. However, none of these approaches provide differential privacy guarantees.

Finally, [37] explores contrastive learning in federated settings but here users feed a user-embedding; the negative samples are created at the server with the differentially private embeddings sent by the users.

## 4 Bounding pairwise-contributions

This section first introduces a condition on the family of loss functions  $\{\ell^{(i,n)}\}$  that, when combined with a clipping operation on the gradient of the similarity between each pair of records, permits the derivation of a DP-SGD variant that benefits from increasing the batch size when using similarity based loss functions.

We start by deriving an expression for the gradient of  $\mathcal{L}$  in lemma 4.1 that

highlights the dependence on the gradient of pairwise similarity values (or logits)  $S(\Phi_w(x_i), \Phi_w(x'_j))$ . By leveraging this decomposition, we find a bound on the overall loss  $\mathcal{L}$  gradient's sensitivity in Theorem 4.2. Finally, we combine these two facts to produce a differentially private optimization algorithm for similarity based loss functions. We defer proofs to the supplementary material.

#### 4.1 Computing gradient sensitivity

Lemma 4.1 below shows that the gradient of a similarity based loss function can be expressed in terms of the pairwise similarity gradients  $\nabla_w S(\Phi_w(x_i), \Phi_w(x'_j))$ .

**Lemma 4.1.** *Let  $\mathcal{L}(w, X) = \sum_{i=1}^n \ell^{(i,n)}(\mathbf{S}^n(\Phi_w(x_i), \Phi_w(\mathbf{x}')))$  be a similarity based loss function as defined in Section 2, then the gradient of  $\mathcal{L}$  with respect to parameter  $w$  is given by*

$$\nabla_w \mathcal{L}(w, X) = \sum_{i=1}^n \sum_{j=1}^n \frac{\partial \ell^{(i,n)}}{\partial Z_{ij}}(\mathbf{S}^n(\Phi_w(x_i), \Phi_w(\mathbf{x}')))) \nabla S(\Phi_w(x_i), \Phi_w(x'_j)) \quad (2)$$

Where  $Z_{ij} = S(\Phi_w(x_i), \Phi_w(x'_j))$

We now describe conditions on the family  $\{\ell^{(i,n)}\}$  function that allow us to derive a bound on the  $L_2$  sensitivity of the  $\mathcal{L}$ 's gradient.

**Theorem 4.2.** *Let  $\mathcal{L}(w, X) = \sum_{i=1}^n \ell^{(i,n)}(\mathbf{S}^n(\Phi_w(x_i), \Phi_w(\mathbf{x}')))$  be a similarity based loss function as defined in Section 2. Let  $\mathcal{C} \subseteq \mathbb{R}$  be a compact set and let  $\mathbf{z}' \in \mathcal{C}^{n-1}$ ,  $z_n \in \mathcal{C}$ , and  $\mathbf{z} = (\mathbf{z}', z_n) \in \mathcal{C}^n$ . Assume that for all  $i \in [n]$  the family of functions  $\{\ell^{(i,n)} : \mathbb{R}^n \rightarrow \mathbb{R}\}_{n \in \mathbb{N}}$  satisfies*

$$\sum_{j=1}^{n-1} \left| \frac{\partial \ell^{(i,n)}}{\partial z_j}(\mathbf{z}) - \frac{\partial \ell^{(i,n-1)}}{\partial z_j}(\mathbf{z}') \right| \leq L \quad (3)$$

$$\sum_{j=1}^n \left| \frac{\partial \ell^{(i,n)}(\mathbf{z})}{\partial z_j} \right| \leq G_1 \quad (4)$$

$$\sum_{i=1}^n \left| \frac{\partial \ell^{(i,n)}(\mathbf{z})}{\partial z_n} \right| \leq G_2 \quad (5)$$

where  $L, G_1$  and  $G_2$  can depend on  $n$ . Assume that  $\|\nabla_w S(\Phi_w(x_i), \Phi_w(x'_j))\|_2 \leq B$ . Then the  $L_2$ -sensitivity of  $\nabla_w \mathcal{L}$  can be bounded as

$$\Delta_2(\nabla_w \mathcal{L}) \leq (G_1 + G_2 + (n-1)L)B$$

We are now in a position to present our main algorithm. The following two corollaries show that one can obtain a private estimate of the gradient of the training loss by doing clipping on pairwise similarity gradients and applying a Gaussian mechanism.

**Corollary 4.3.** Let  $B > 0$ ,  $z \in \mathbb{R}^d$  and  $\text{Clip}_B(x) = \min(B/\|x\|, 1)x$  denote the vector  $x$  clipped to have norm at most  $B$ . Suppose the family of functions  $\ell^{(i,n)}$  satisfy the conditions of Theorem 4.2. Then, the function

$$\mathbf{X} \mapsto \sum_{i=1}^n \sum_{j=1}^n \frac{\partial \ell^{(i,n)}}{\partial Z_{ij}} (\mathbf{S}^n(\Phi_w(x_i), \Phi_w(\mathbf{x}')) \text{Clip}_B(\nabla \text{S}(\Phi_w(x_i), \Phi_w(x'_j)))) \quad (6)$$

has  $L_2$  sensitivity bounded by  $(G_1 + G_2 + (n-1)L)B$ .

**Corollary 4.4.** If the family of loss functions  $\ell^{(i,n)}$  satisfies the conditions of Theorem 4.2, then each iteration of Algorithm 1 satisfies  $(\epsilon, \delta)$ -differential privacy for  $\epsilon = \sqrt{\log(1.25/\delta)}/\sigma$ <sup>1</sup>

*Proof.* The proof is immediate since each step of the algorithm corresponds to the Gaussian mechanism with noise calibrated to the sensitivity of the mechanism.  $\square$

An observant reader may point out that our sensitivity bound has a dependence on  $n$  that is undesirable, as our algorithm would seem to add as much noise as a naive implementation of DP-SGD. In the following lemmas, we show that for commonly used losses like the contrastive loss and spreadout regularizer loss, condition (3) happens to hold with  $L = O(1/n)$ . Consequently, this ensures that the total sensitivity remains constant as the number of examples in batch increases.

**Lemma 4.5.** Let  $\ell^{(i,n)}$  denote the contrastive loss of example 1. Then  $\ell^{(i,n)}$  satisfies the conditions of Theorem 4.2 for

$$G_1 + G_2 + (n-1)L \leq 2 \left( 1 + \frac{(n-2)e^2}{e^2 + (n-1)} \right) \quad (7)$$

**Lemma 4.6.** Let  $\ell^{(i,n)}$  denote the spreadout regularizer of example 2. Then  $\ell^{(i,n)}$  satisfies the conditions of Theorem 4.2 for

$$G_1 + G_2 + (n-1)L \leq 6$$

*Proof.* By definition the spreadout loss is given by:

$$\ell^{(i,n)}(\mathbf{z}) = \frac{1}{n-1} \sum_{j \neq i}^n z_j^2$$

We now calculate the values of  $L, G_1, G_2$  that make this function satisfy the conditions of Theorem 4.2. Let  $\mathbf{z} = (\mathbf{z}', z_n)$  then we have that

$$\frac{\partial \ell^{(i,n)}(\mathbf{z})}{\partial z_j} - \frac{\partial \ell^{(i,n-1)}(\mathbf{z}')}{\partial z_j} = \frac{2}{n-1} z_j - \frac{2}{n-2} z_j = -\frac{2}{(n-1)(n-2)} z_j$$

<sup>1</sup>A slightly tighter relation between  $\sigma$  and  $\epsilon$  can be given using the results on the analytic Gaussian mechanism of [4].



for  $j \neq i$  and 0 otherwise. Let  $C \leq \max_{j=1\dots n} z_j$  we then have:

$$\sum_{j=1}^{n-1} \left| \frac{\partial \ell^{(i,n)}(\mathbf{z})}{\partial z_j} - \frac{\partial \ell^{(i,n-1)}(\mathbf{z}')}{\partial z_j} \right| \leq \sum_{j \neq i}^{n-1} \frac{2}{(n-1)(n-2)} |z_j| \leq \frac{2C}{n-1} =: L$$

Similarly we have

$$\sum_{j=1}^n \frac{\partial \ell^{(n,n)}(\mathbf{z})}{\partial z_j} \leq 2C =: G_1 \quad \text{and} \quad \sum_{i=1}^n \frac{\partial \ell^{(i,n)}(\mathbf{z})}{\partial z_j} \leq 2C =: G_2$$

Therefore we have that

$$G_1 + G_2 + (n-1)L \leq 6C$$

Finally, note that the input to the spreaduout regularizer is given by  $z_{ij} = S(\Phi(x_i), \Phi(x'_j))$  where the S corresponds to the cosine similarity. Therefore we must have that  $C = 1$  and the result follows.  $\square$

## 4.2 Main algorithm

We introduce our proposed private optimization routine as algorithm 1. The algorithm receives as input standard constants batch size  $n$ , learning rate (or schedule)  $\eta$ , and a number of iterations  $T$ . In addition, it receives constants  $G_1$ ,  $G_2$ , and  $L$  defined in theorem 4.2, and the similarity gradient clip norm  $B$ , and computes the sensitivity of the overall gradient  $C$  (line 2).

The algorithm proceeds to the training loop where at each iteration  $t$  samples a batch of size  $n$ . Then, instead of per-example gradients, computes similarity gradients  $g_{ij}$  (line 5), clips all  $g_{ij}$ 's to obtain bounded sensitivity  $\bar{g}_{ij}$ , and computes an approximate gradient for  $\mathcal{L}$  using eq. (6) (line 7). Finally, it applies noise (line 8) and updates the model (line 9).

We would like to remark that all previous work on privacy accounting for DP-SGD also applies to our algorithm as each iteration simply generates a private version of the gradient of the batch loss.

## 5 Numerical Experiments

This section presents numerical experiments that compare the practical viability of our proposed DP-SGD variant (Logit-DP), the implementation of DP-SGD (Naive-DP) which clips the aggregated gradient at the batch level, and non-private SGD (Non-Private). Specifically, we examined several training and testing metrics on pre-training and fine-tuning tasks applied to the CIFAR10 and CIFAR100 datasets. For conciseness, the details of the embedding models, the hyperparameters of the each variants, and the training setups for each task are given in the Appendix.

The last subsection also describes some memory scaling issues that we encountered during training and some possible remedies to these issues.

---

**Algorithm 1:** Logit-DP, a DP-SGD algorithm for similarity based non-decomposable loss functions.

---

**Input:** Similarity gradient clip norm  $B$ , constants  $G_1, G_2$ , and  $L$  in theorem 4.2, dataset  $D = \{(x_i, x'_i)\}_{i=1}^N$ , batch size  $n$ , number of iterations  $T$ , learning rate  $\eta$ , noise multiplier  $\sigma$ , model architecture  $\Phi$

**Output:** Embedding model  $\Phi_{w_T}$

```

1 initialize  $w_0 \in \mathbb{R}^p$ ;
2 Compute gradient sensitivity  $C = (G_1 + G_2 + nL)B$ ;
3 for  $t = 0, 2, \dots, T - 1$  do
4   Sample batch  $X = \{(x_1, x'_1), \dots, (x_n, x'_n)\}$ ;
5   Compute similarity gradients  $g_{ij} = \nabla_{w_t} S(\Phi_{w_t}(x_i), \Phi_{w_t}(x'_j))$ ;
6   Clip gradients  $\bar{g}_{ij} = \min \left\{ \frac{B}{\|g_{ij}\|}, 1 \right\} g_{ij}$ ;
7   Compute approximate gradient  $\bar{g}$  using (6).;
8   Compute noisy gradient  $\tilde{g} = \bar{g} + Y$  for  $Y \sim \mathcal{N}(0, \sigma C I_p)$ .;
9   Update the model  $w_{t+1} = w_t - \eta \tilde{g}$ .;
10 end

```

---

## 5.1 Pre-training on CIFAR10

In these experiments, all DP-SGD and SGD variants were given a common embedding model  $\Phi$  and were tasked with minimizing the contrastive loss described in Example 1 for the examples in the CIFAR10 dataset. For testing/evaluation metrics, we examined the quality of the embedding model under a  $k$ -nearest neighbors ( $k$ -NN) for  $k = 3$ .

Figure 1 presents the observed (relative) training loss values over the number of examples seen so far for ten different training runs, and Table 1 presents the relative averaged test metrics at the last evaluation point.

Table 1: Relative aggregate CIFAR10 test metrics generated by the confusion matrix  $C$  at the last test point over ten runs. Each aggregate metric is divided by the corresponding one for Non-Private. Aggregate accuracy is defined as  $\sum_i C_{ii} / \sum_{i,j} C_{ij}$  averaged over all runs. The top recall, precision, and  $F_\beta$  scores are the average of the best observed metric over all ten CIFAR10 classes.

|             | Relative Test Metrics |            |               |                     |
|-------------|-----------------------|------------|---------------|---------------------|
|             | Accuracy              | Top Recall | Top Precision | Top $F_\beta$ Score |
| Logit-DP    | 0.742                 | 0.805      | 0.786         | 0.791               |
| Naive-DP    | 0.563                 | 0.575      | 0.575         | 0.576               |
| Non-Private | 1.000                 | 1.000      | 1.000         | 1.000               |

For reference, we present each variant’s confusion matrices and (absolute) averaged test metrics — at the last evaluation point — in Figure 3 and Table 3 of the Appendix, respectively.

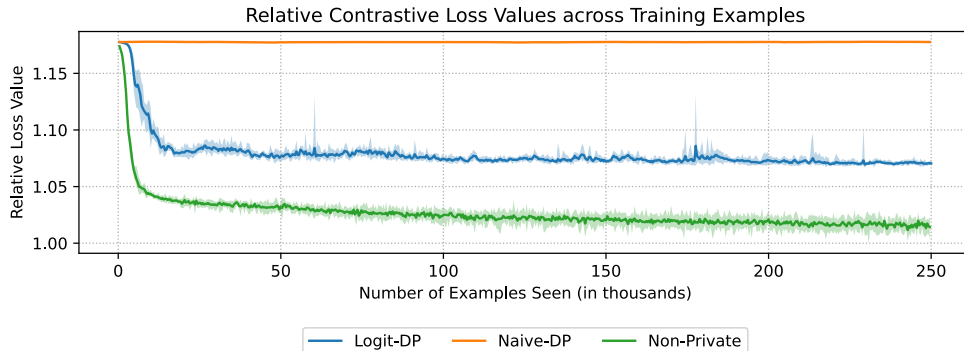


Figure 1: Relative CIFAR10 training loss over ten runs. Relative loss is defined as the observed training loss divided by the minimum loss observed across all runs and all variants. Shaded regions bound the observed loss values over the runs, while the dark lines represent the average relative loss observed so far.

## 5.2 Fine-tuning on CIFAR100

Pretrained foundational models are often non-privately fine-tuned on classification tasks for local use and consequently are not required to be privately optimized. In these experiments, we test the ability of the privately pre-trained embedding model to adapt to new tasks. All variants were given their pretrained model  $\Phi$  from Subsection 5.1 and a multilayer full-connected model  $\Psi$ . They were then tasked with non-privately minimizing the cross-entropy loss generated by the combined model  $\Phi \circ \Psi$  on the CIFAR100 dataset to predict the coarse label of the input (20 categories), under the condition that the weights in  $\Phi$  were frozen, i.e., could not be updated.

Table 2: Relative CIFAR100 test metrics generated by the confusion matrix  $C$  at the last test point over one run. Each metric is divided by the corresponding one for non-private DP-SGD (Non-Private). Accuracy is defined as  $\sum_i C_{ii} / \sum_{i,j} C_{ij}$  while top recall, precision, and  $F_\beta$  scores are the best observed metric over all CIFAR100 classes.

|             | Relative Test Metrics |            |               |                     |
|-------------|-----------------------|------------|---------------|---------------------|
|             | Accuracy              | Top Recall | Top Precision | Top $F_\beta$ Score |
| Logit-DP    | 0.855                 | 0.806      | 0.569         | 0.699               |
| Naive-DP    | 0.721                 | 0.995      | 0.485         | 0.672               |
| Non-Private | 1.000                 | 1.000      | 1.000         | 1.000               |

For reference, we present each variant’s (absolute) test metrics — at the last evaluation point — in Table 4 of the Appendix.

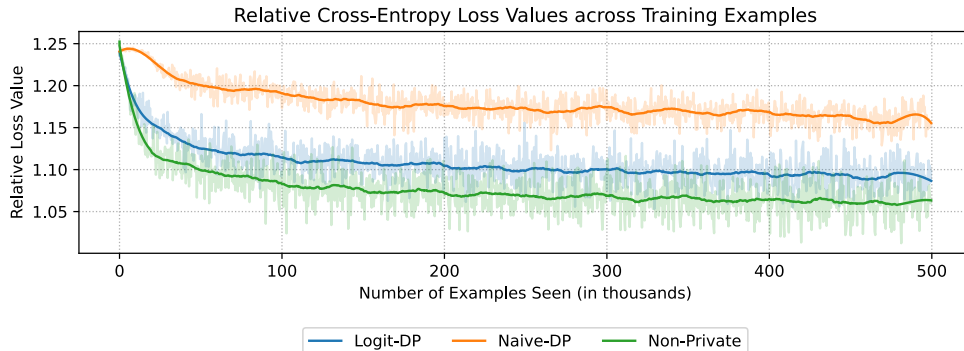


Figure 2: Relative CIFAR100 training loss for a single run. Relative loss is defined as the observed training loss divided by the minimum loss observed across all variants. Lightly colored lines are the true loss values, while the dark lines are smoothed loss values generated by a third-order Savitzky-Golay filter with a sliding window of 100 observations.

### 5.3 A memory bottleneck and a potential fix

In our implementation of Logit-DP (Algorithm 1), one of our noticeable computational bottlenecks was the materialization of the  $n^2$  logit gradients ( $g_{ij}$  in Algorithm 1) for a batch  $n$  examples, which were needed to compute the final aggregated gradient ( $\bar{g}$  in Algorithm 1). Specifically, due to the large  $\Theta(n^2|w|)$  memory cost of computing these gradients, we were unable to test our proposed approach on larger embedding models  $\Phi_w$  during pre-training.

A potential solution is to compute gradients  $g_{ij}$  sequentially. While addressing the memory bottleneck, this solution is computationally slow.

Below, we describe an alternative approach for computing  $\bar{g}$  and argue that it is more efficient for certain choices  $\Phi_w$ . Consider the function

$$F_X(w) := \sum_{i=1}^n \sum_{j=1}^n \lambda_{ij} \mathbf{S}^n(\Phi_w(x_i), \Phi_w(x'_j))$$

where  $\lambda_{ij}$  are fixed, real-valued weights given by

$$\tau_{ij} := \frac{\partial \ell^{(i,n)}}{\partial Z_{ij}}(\mathbf{S}^n(\Phi_w(x_i), \Phi_w(x'_j))), \quad \lambda_{ij} := \tau_{ij} \min \left\{ \frac{B}{\|g_{ij}\|}, 1 \right\} \quad \forall i, j,$$

and note that  $\bar{g} = \nabla F_X(w)$  (cf. (6)). In view of the previous identity, an alternative approach to computing  $\bar{g}$  is to first compute each  $\lambda_{ij}$  and *then* compute  $\nabla F_X(w)$ .

This new approach has the following advantages: (i) given  $\lambda_{ij}$ , the memory and runtime cost of computing the gradient of  $F_X(w)$  is on the same order of magnitude as computing the gradient of  $\mathcal{L}(w, X) = \sum_{i=1}^n \ell^{(i,n)}(\mathbf{S}^n(\Phi_w(x_i), \Phi_w(\mathbf{x}')))$  when both methods employ backpropagation, (ii) the memory cost of storing

the weights  $\lambda_{ij}$  is only  $\Theta(n^2)$ , and (iii) the costs of computing the weights  $\lambda_{ij}$  requires only computing the  $n^2$  scalar pairs  $(\tau_{ij}, \|g_{ij}\|)$  rather than computing the  $n^2$  gradients  $g_{ij}$  of size  $|w|$  as in Algorithm 1.

The last advantage is of particular interest, as there are well-known methods [15, 31, 21] in the literature to efficiently computing the norms  $\|g_{ij}\|$  without materializing each  $g_{ij}$ . Specifically, most of these methods involve decomposing  $g_{ij}$  into some low-rank representation  $g_{ij} = U_{ij}V_{ij}^\top$  for low-rank matrices  $U_{ij}$  and  $V_{ij}$ , and then exploiting the identity

$$\|g_{ij}\|^2 = \|U_{ij}V_{ij}^\top\|^2 = \langle U_{ij}^\top U_{ij}, V_{ij}^\top V_{ij} \rangle.$$

For example, when  $U_{ij}$  and  $V_{ij}$  are column vectors, then the last expression above reduces to  $\|U_{ij}\|^2\|V_{ij}\|^2$ , which can be substantially more efficient than first materializing  $g_{ij} = U_{ij}V_{ij}^\top$  and then computing  $\|g_{ij}\|$ . A correct implementation of this technique is far from trivial and we leave this as future research in this exciting area of privacy.

## 6 Discussion

As observed in section 3, naive implementations of DP-SGD for similarity based losses is ineffective because the standard deviation of the noise in the gaussian mechanism grows with  $n$ . Experiments in the previous section show that even with careful hyperparameter tuning, the loss remains almost constant during pre-training. Fine-tuned models also perform poorly compared to both the non-private baseline and the Logit-DP algorithm.

Careful analysis of these losses and their decomposition shows that by clipping logit gradients, Logit-DP obtains a sensitivity that is constant on the batch size, considerably reducing the magnitude of the noise added to privatize the gradient. These insights expand the suite of tasks that can be trained in a privacy preserving way with little accuracy drop. Work on efficient implementation of these algorithms is an interesting avenue of future work and we introduce concrete ideas at the end of the previous section.

## References

- [1] Midjourney. [midjourney.com](https://www.midjourney.com). Accessed: 2023-05-11.
- [2] Martin Abadi, Andy Chu, Ian Goodfellow, H Brendan McMahan, Ilya Mironov, Kunal Talwar, and Li Zhang. Deep learning with differential privacy. In *Conference on Computer and Communications Security (SIGSAC)*, 2016.
- [3] Borja Balle, Giovanni Cherubin, and Jamie Hayes. Reconstructing training data with informed adversaries. In *2022 IEEE Symposium on Security and Privacy (SP)*. IEEE, 2022.

- [4] Borja Balle and Yu-Xiang Wang. Improving the Gaussian mechanism for differential privacy: Analytical calibration and optimal denoising. In *International Conference on Machine Learning (ICML)*, 2018.
- [5] Andrea Banino, Adrià Puidomenech Badia, Jacob Walker, Tim Scholtes, Jovana Mitrovic, and Charles Blundell. Coberl: Contrastive bert for reinforcement learning. *arXiv preprint arXiv:2107.05431*, 2021.
- [6] Kamalika Chaudhuri, Claire Monteleoni, and Anand D Sarwate. Differentially private empirical risk minimization. *Journal of Machine Learning Research*, 2011.
- [7] Ting Chen, Simon Kornblith, Mohammad Norouzi, and Geoffrey Hinton. A simple framework for contrastive learning of visual representations. In *International Conference on Machine Learning (ICML)*, 2020.
- [8] Ting Chen, Simon Kornblith, Kevin Swersky, Mohammad Norouzi, and Geoffrey E Hinton. Big self-supervised models are strong semi-supervised learners. *Advances in neural information processing systems*, 33, 2020.
- [9] Muthuraman Chidambaram, Yinfei Yang, Daniel Cer, Steve Yuan, Yun-Hsuan Sung, Brian Strope, and Ray Kurzweil. Learning cross-lingual sentence representations via a multi-task dual-encoder model. *arXiv preprint arXiv:1810.12836*, 2018.
- [10] Jacob Devlin, Ming-Wei Chang, Kenton Lee, and Kristina Toutanova. BERT: Pre-training of deep bidirectional transformers for language understanding. In *Conference of the North American Chapter of the Association for Computational Linguistics: Human Language Technologies*, 2019.
- [11] Cynthia Dwork, Frank McSherry, Kobbi Nissim, and Adam Smith. Calibrating noise to sensitivity in private data analysis. In *Theory of cryptography conference*, 2006.
- [12] Hongchao Fang, Sicheng Wang, Meng Zhou, Jiayuan Ding, and Pengtao Xie. Cert: Contrastive self-supervised learning for language understanding. *arXiv preprint arXiv:2005.12766*, 2020.
- [13] Badih Ghazi, Pasin Manurangsi, Pritish Kamath, Ravi Kumar Ravikumar, and Vadym Doroshenko. Connect the dots: Tighter discrete approximations of privacy loss distributions. *arXiv preprint arXiv:2207.04380*, 2022.
- [14] John Giorgi, Osvald Nitski, Bo Wang, and Gary Bader. Declutr: Deep contrastive learning for unsupervised textual representations. *arXiv preprint arXiv:2006.03659*, 2020.
- [15] Ian Goodfellow. Efficient per-example gradient computations. *arXiv preprint arXiv:1510.01799*, 2015.

- [16] Xinlei He and Yang Zhang. Quantifying and mitigating privacy risks of contrastive learning. In *Conference on Computer and Communications Security (SIGSAC)*, 2021.
- [17] Mengdi Huai, Di Wang, Chenglin Miao, Jinhui Xu, and Aidong Zhang. Pairwise learning with differential privacy guarantees. *Conference on Artificial Intelligence (AAAI)*, 34, 2020.
- [18] Yilin Kang, Yong Liu, Jian Li, and Weiping Wang. Towards sharper utility bounds for differentially private pairwise learning. *arXiv preprint arXiv:2105.03033*, 2021.
- [19] Anastasia Koloskova, Hadrien Hendrikx, and Sebastian U Stich. Revisiting gradient clipping: Stochastic bias and tight convergence guarantees. *arXiv preprint arXiv:2305.01588*, 2023.
- [20] Fabian Latorre, Paul Rolland, and Volkan Cevher. Lipschitz constant estimation of neural networks via sparse polynomial optimization. In *International Conference on Learning Representations (ICLR)*, 2020.
- [21] Jaewoo Lee and Daniel Kifer. Scaling up differentially private deep learning with fast per-example gradient clipping. *arXiv preprint arXiv:2009.03106*, 2020.
- [22] Wenjun Li, Anli Yan, Di Wu, Taoyu Zhu, Teng Huang, Xuandi Luo, and Shaowei Wang. Dpcl: Contrastive representation learning with differential privacy. *International Journal of Intelligent Systems*, 2022.
- [23] Xuechen Li, Florian Tramer, Percy Liang, and Tatsunori Hashimoto. Large language models can be strong differentially private learners. *arXiv preprint arXiv:2110.05679*, 2021.
- [24] Hongbin Liu, Jinyuan Jia, Wenjie Qu, and Neil Zhenqiang Gong. Encodermi: Membership inference against pre-trained encoders in contrastive learning. In *Conference on Computer and Communications Security (SIGSAC)*, 2021.
- [25] Lajanugen Logeswaran and Honglak Lee. An efficient framework for learning sentence representations. *arXiv preprint arXiv:1803.02893*, 2018.
- [26] Vien V Mai and Mikael Johansson. Stability and convergence of stochastic gradient clipping: Beyond lipschitz continuity and smoothness. In *International Conference on Machine Learning (ICML)*, 2021.
- [27] Ilya Mironov. Rényi differential privacy. In *IEEE computer security foundations symposium (CSF)*, 2017.
- [28] Alec Radford, Jong Wook Kim, Chris Hallacy, Aditya Ramesh, Gabriel Goh, Sandhini Agarwal, Girish Sastry, Amanda Askell, Pamela Mishkin, Jack Clark, et al. Learning transferable visual models from natural language

- supervision. In *International Conference on Machine Learning (ICML)*, 2021.
- [29] Alec Radford, Karthik Narasimhan, Tim Salimans, Ilya Sutskever, et al. Improving language understanding by generative pre-training. 2018.
- [30] Shideh Rezaeifar, Slava Voloshynovskiy, Meisam Asgari Jirhandeh, and Vitality Kinakh. Privacy-preserving image template sharing using contrastive learning. *Entropy*, 2022.
- [31] Gaspar Rochette, Andre Manoel, and Eric W Tramel. Efficient per-example gradient computations in convolutional neural networks. *arXiv preprint arXiv:1912.06015*, 2019.
- [32] Chitwan Saharia, William Chan, Saurabh Saxena, Lala Li, Jay Whang, Emily L Denton, Kamyar Ghasemipour, Raphael Gontijo Lopes, Burcu Karagol Ayan, Tim Salimans, et al. Photorealistic text-to-image diffusion models with deep language understanding. *Advances in Neural Information Processing Systems*, 2022.
- [33] Zhouxing Shi, Yihan Wang, Huan Zhang, J Zico Kolter, and Cho-Jui Hsieh. Efficiently computing local lipschitz constants of neural networks via bound propagation. *Advances in Neural Information Processing Systems*, 2022.
- [34] Reza Shokri, Marco Stronati, Congzheng Song, and Vitaly Shmatikov. Membership inference attacks against machine learning models. In *2017 IEEE symposium on security and privacy (SP)*. IEEE, 2017.
- [35] Congzheng Song and Ananth Raghunathan. Information leakage in embedding models. In *Conference on Computer and Communications Security (SIGSAC)*, 2020.
- [36] Romal Thoppilan, Daniel De Freitas, Jamie Hall, Noam Shazeer, Apoorv Kulshreshtha, Heng-Tze Cheng, Alicia Jin, Taylor Bos, Leslie Baker, Yu Du, et al. LaMDA: Language Models for Dialog Applications. *arXiv preprint arXiv:2201.08239*, 2022.
- [37] Chuhan Wu, Fangzhao Wu, Tao Qi, Yongfeng Huang, and Xing Xie. Fedcl: Federated contrastive learning for privacy-preserving recommendation. *arXiv preprint arXiv:2204.09850*, 2022.
- [38] Zhuofeng Wu, Sinong Wang, Jiatao Gu, Madian Khabsa, Fei Sun, and Hao Ma. Clear: Contrastive learning for sentence representation. *arXiv preprint arXiv:2012.15466*, 2020.
- [39] Zheng Xu, Maxwell Collins, Yuxiao Wang, Liviu Panait, Sewoong Oh, Sean Augenstein, Ting Liu, Florian Schroff, and H Brendan McMahan. Learning to generate image embeddings with user-level differential privacy. *arXiv preprint arXiv:2211.10844*, 2022.



- [40] Zhiyu Xue, Shaoyang Yang, Mengdi Huai, and Di Wang 0015. Differentially private pairwise learning revisited. In *IJCAI*, 2021.
- [41] Zhenhuan Yang, Yunwen Lei, Siwei Lyu, and Yiming Ying. Stability and differential privacy of stochastic gradient descent for pairwise learning with non-smooth loss. In *Conference on Artificial Intelligence and Statistics (AISTATS)*, 2021.
- [42] Felix Yu, Ankit Singh Rawat, Aditya Menon, and Sanjiv Kumar. Federated learning with only positive labels. In *International Conference on Machine Learning (ICML)*, 2020.
- [43] Xu Zhang, Felix X Yu, Sanjiv Kumar, and Shih-Fu Chang. Learning spread-out local feature descriptors. In *IEEE International Conference on Computer Vision*, 2017.

# Supplementary material for DP-SGD for non-decomposable objective functions

## A Proofs

**Theorem.** [theorem 4.2] Let  $\mathcal{L}(w, X) = \sum_{i=1}^n \ell^{(i,n)}(\mathbf{S}^n(\Phi_w(x_i), \Phi_w(\mathbf{x}')))$  be a similarity based loss function as defined in Section 2. Let  $\mathcal{C} \subseteq \mathbb{R}$  be a compact set and let  $\mathbf{z}' \in \mathcal{C}^{n-1}$ ,  $z_n \in \mathcal{C}$ , and  $\mathbf{z} = (\mathbf{z}', z_n) \in \mathcal{C}^n$ . Assume that for all  $i \in [n]$  the family of functions  $\{\ell^{(i,n)} : \mathbb{R}^n \rightarrow \mathbb{R}\}_{n \in \mathbb{N}}$  satisfies

$$\sum_{j=1}^{n-1} \left| \frac{\partial \ell^{(i,n)}}{\partial z_j}(\mathbf{z}) - \frac{\partial \ell^{(i,n-1)}}{\partial z_j}(\mathbf{z}') \right| \leq L \quad (8)$$

$$\sum_{j=1}^n \left| \frac{\partial \ell^{(i,n)}(\mathbf{z})}{\partial z_j} \right| \leq G_1 \quad (9)$$

$$\sum_{i=1}^n \left| \frac{\partial \ell^{(i,n)}(\mathbf{z})}{\partial z_n} \right| \leq G_2 \quad (10)$$

where  $L, G_1$  and  $G_2$  can depend on  $n$ . Assume that  $\|\nabla_w \mathbf{S}(\Phi_w(x_i), \Phi_w(x'_j))\|_2 \leq B$ . Then the  $L_2$ -sensitivity of  $\nabla_w \mathcal{L}$  can be bounded as

$$\Delta_2(\nabla_w \mathcal{L}) \leq (G_1 + G_2 + (n-1)L)B$$

**Proof. Notation.** Given a function  $f : \mathbb{R}^m \rightarrow \mathbb{R}^n$ , let  $D_x f(x)$  denote the jacobian matrix of  $f$  (with respect to variable  $x$ ) at point  $x \in \mathbb{R}^m$ , where the  $i, j$  entry is defined as  $\frac{\partial f_i}{\partial x_j}$ .

For  $j \in [n]$  let  $Z_{i,j}(w) = \mathbf{S}(\Phi_w(x_i), \Phi_w(x_j))$ . When clear from context we write  $Z_{ij}$  and drop the dependence on  $w$ . Let  $\mathbf{Z}'_i = (Z_{i1}, \dots, Z_{i,n-1}) = \mathbf{S}^{n-1}(\Phi_w(x_i), \Phi_w(\mathbf{x}')) \in \mathbb{R}^{n-1}$  and  $\mathbf{Z}_i = \mathbf{S}^n(\Phi_w(x_i), \Phi_w(\mathbf{x}'))$ . The gradient of  $\mathcal{L}$  respect to  $w$  on batch  $\{(x_i, x'_i)\}_{i=1}^n$  can be computed using the chain rule as

$$\nabla_w \mathcal{L}(w, X) = \sum_{i=1}^n D_{\mathbf{Z}_i} \ell^{(i,n)}(\mathbf{Z}_i) \mathbf{D}_w \mathbf{S}^n(\Phi_w(\mathbf{x}_i), \Phi_w(\mathbf{x}')) \quad (11)$$

$$(12)$$

Since  $\ell^{(i,n)}$  is a scalar function,  $D$  is the gradient operator. Therefore, we have that

$$D_{\mathbf{Z}} \ell^{(i,n)}(\mathbf{Z}_i) = \nabla_{\mathbf{Z}_i} \ell^{(i,n)}(\mathbf{Z}_i)^\top \in \mathbb{R}^{1 \times n}.$$

Similarly, we have that

$$D \mathbf{S}^n(\Phi_w(x_i), \Phi_w(\mathbf{x}')) = \begin{bmatrix} \nabla \mathbf{S}(\Phi_w(x_i), \Phi_w(x'_1))^\top \\ \vdots \\ \nabla \mathbf{S}(\Phi_w(x_i), \Phi_w(x'_n))^\top \end{bmatrix}.$$

Consequently, the expression for the gradient of  $\mathcal{L}$  in eq. (11) can be reduced to

$$\nabla_w \mathcal{L}(w, X) = \sum_{i=1}^n \sum_{j=1}^n \frac{\partial \ell^{(i,n)}(\mathbf{Z}_i)}{\partial Z_{ij}} \nabla S(\Phi_w(x_i), \Phi_w(x'_j))$$

We can use this expression to bound the sensitivity of the gradient. Let  $\mathcal{D} = \{(x_i, x'_i)\}_{i=1}^n$  and  $\mathcal{D}' = \{(x_i, x'_i)\}_{i=1}^{n-1}$  be two datasets differing on record  $(x_n, x'_n)$ . The  $\ell_2$  sensitivity of the gradient of  $\mathcal{L}$  respect to  $w$  on datasets  $\mathcal{D}$  and  $\mathcal{D}'$  can be expressed as

$$\Delta_2(\nabla \mathcal{L}) = \left\| \sum_{i=1}^n \sum_{j=1}^n \frac{\partial \ell^{(i,n)}(\mathbf{Z}_i)}{\partial Z_{ij}} \nabla S(\Phi_w(x_i), \Phi_w(x'_j)) - \sum_{i=1}^{n-1} \sum_{j=1}^{n-1} \frac{\partial \ell^{(i,n-1)}(\mathbf{Z}'_i)}{\partial Z_{ij}} \nabla S(\Phi_w(x_i), \Phi_w(x'_j)) \right\|$$

The above expression can be broken down into the following terms:

$$\begin{aligned} \Delta_2(\nabla \mathcal{L}) = & \left\| \underbrace{\sum_{j=1}^n \frac{\partial \ell^{(n,n)}(Z_n)}{\partial Z_{n,j}} \nabla S(\Phi_w(x_n), \Phi_w(x'_j))}_{T_1} + \underbrace{\sum_{i=1}^{n-1} \frac{\partial \ell^{(i,n)}(\mathbf{Z}_i)}{\partial Z_{i,n}} \nabla S(\Phi_w(x_i), \Phi_w(x'_n))}_{T_2} \right. \\ & \left. + \sum_{i=1}^{n-1} \sum_{j=1}^{n-1} \underbrace{\left( \frac{\partial \ell^{(i,n)}(\mathbf{Z}_i)}{\partial Z_{ij}} - \frac{\partial \ell^{(i,n-1)}(\mathbf{Z}'_i)}{\partial Z_{ij}} \right) \nabla S(\Phi_w(x_i), \Phi_w(x'_j))}_{T_3} \right\|. \end{aligned}$$

We use triangle inequality and bound independently each term.

$$\begin{aligned} \|T_1\| &= \left\| \sum_{j=1}^n \frac{\partial \ell^{(n,n)}(Z_n)}{\partial Z_{n,j}} \nabla S(\Phi_w(x_n), \Phi_w(x'_j)) \right\| \\ &\leq \sum_{j=1}^n \left| \frac{\partial \ell^{(n,n)}(Z_n)}{\partial Z_{n,j}} \right| \|\nabla S(\Phi_w(x_n), \Phi_w(x'_j))\| \\ &\leq \sum_{j=1}^n \left| \frac{\partial \ell^{(n,n)}(Z_n)}{\partial Z_{n,j}} \right| B \\ &\leq G_1 B \end{aligned}$$

Where we used the triangle inequality on the first step and the assumed bounds on  $S(\Phi_w(x_n), \Phi_w(x'_j))$  and the family of losses  $\ell^{(i,n)}$  for the third and last steps.

Analogously we obtain

$$\begin{aligned} \|T_2\| &= \left\| \sum_{i=1}^{n-1} \frac{\partial \ell^{(i,n)}(\mathbf{Z}_i)}{\partial Z_{i,n}} \nabla S(\Phi_w(x_i), \Phi(x'_n)) \right\| \\ &\leq G_2 B \end{aligned}$$

Finally, using the assumption on the partial derivatives of the family  $\{\ell^{(i,n)}\}_{n \in \mathbb{N}}$

$$\begin{aligned} \|T_3\| &= \left\| \sum_{i=1}^{n-1} \sum_{j=1}^{n-1} \left( \frac{\partial \ell^{(i,n)}(\mathbf{Z}_i)}{\partial Z_{i,j}} - \frac{\partial \ell^{(i,n-1)}(\mathbf{Z}_i)}{\partial Z_{i,j}} \right) \nabla S(\Phi_w(x_i), \Phi_w(x'_j)) \right\| \\ &\leq \sum_{i=1}^{n-1} \sum_{j=1}^{n-1} \left| \frac{\partial \ell^{(i,n)}(\mathbf{Z}_i)}{\partial Z_{i,j}} - \frac{\partial \ell^{(i,n-1)}(\mathbf{Z}_i)}{\partial Z_{i,j}} \right| \|\nabla S(\Phi_w(x_i), \Phi_w(x'_j))\| \\ &\leq \sum_{i=1}^{n-1} \sum_{j=1}^{n-1} \left| \frac{\partial \ell^{(i,n)}(\mathbf{Z}_i)}{\partial Z_{i,j}} - \frac{\partial \ell^{(i,n-1)}(\mathbf{Z}_i)}{\partial Z_{i,j}} \right| B \\ &= \sum_{i=1}^{n-1} B \sum_{j=1}^{n-1} \left| \frac{\partial \ell^{(i,n)}(\mathbf{Z}_i)}{\partial Z_{i,j}} - \frac{\partial \ell^{(i,n-1)}(\mathbf{Z}_i)}{\partial Z_{i,j}} \right| \\ &\leq (n-1)BL \end{aligned}$$

and combining the three expressions we obtain

$$\Delta_2(\nabla_w L) \leq (G_1 + G_2)B + (n-1)LB$$

□

*Proof.* The proof follows immediatly from theorem 4.2. □

**Lemma.** lemma 4.5 Let  $\ell^{(i,n)}$  denote the contrastive loss of example 1. Then  $\ell^{(i,n)}$  satisfies the conditions of Theorem 4.2 for

$$G_1 + G_2 + (n-1)L \leq 2 \left( 1 + \frac{(n-2)e^2}{e^2 + (n-1)} \right) \quad (13)$$

*Proof.* Recall the family of functions used for the contrastive loss in section 2,

$$\ell^{(i,n)}(\mathbf{z}) = \log \left( \sum_{j=1}^n e^{z_j} \right) - z_i.$$

In this case,

$$\frac{\partial \ell^{(i,n)}(z_1, \dots, z_n)}{\partial z_j} = \begin{cases} \frac{e^{z_i}}{\sum_{k=1}^n z_k} - 1 & \text{if } j = i \\ \frac{e^{z_j}}{\sum_{k=1}^n e^{z_k}} & \text{otherwise.} \end{cases}$$

We can derive that

$$\sum_{j=1}^n \left| \frac{\partial \ell^{(n,n)}(z_1, \dots, z_n)}{\partial z_j} \right| = \sum_{j=1}^{n-1} \frac{e^{z_j}}{\sum_{k=1}^n e^{z_k}} + \left( 1 - \frac{e^{z_n}}{\sum_{k=1}^n e^{z_k}} \right)$$

Note that  $\sum_{j=1}^{n-1} \frac{e^{z_j}}{\sum_{k=1}^n e^{z_k}} = 1 - \frac{e^{z_n}}{\sum_{k=1}^n e^{z_k}}$ , since the  $n$  terms constitute a probability distribution summing up to 1, thus

$$\begin{aligned} \sum_{j=1}^n \left| \frac{\partial \ell^{(n,n)}(z_1, \dots, z_n)}{\partial z_j} \right| &= \left( 1 - \frac{e^{z_n}}{\sum_{k=1}^n e^{z_k}} \right) + \left( 1 - \frac{e^{z_n}}{\sum_{k=1}^n e^{z_k}} \right) \\ &= 2 \left( 1 - \frac{e^{z_n}}{\sum_{k=1}^n e^{z_k}} \right) \end{aligned}$$

Letting  $p_n = \frac{e^{z_n}}{\sum_{k=1}^n e^{z_k}}$ , we have that

$$G_1 = \sum_{j=1}^n \left| \frac{\partial \ell^{(n,n)}(z_1, \dots, z_n)}{\partial z_j} \right| = 2(1 - p_n) \quad (14)$$

$$(15)$$

Next we look into  $G_2 = \sum_{i=1}^{n-1} \left| \frac{\partial \ell^{(i,n)}(z_1, \dots, z_n)}{\partial z_n} \right|$ . In this case,

$$\begin{aligned} \sum_{i=1}^{n-1} \left| \frac{\partial \ell^{(i,n)}(z_1, \dots, z_n)}{\partial z_n} \right| &= \sum_{i=1}^{n-1} \frac{e^{z_n}}{\sum_{k=1}^n e^{z_k}} \\ &= \frac{(n-1)e^{z_n}}{\sum_{k=1}^n e^{z_k}} \end{aligned} \quad (16)$$

yielding

$$G_2 = (n-1)p_n. \quad (17)$$

Finally, for the condition on the difference we have that for all  $i \in [n]$ ,

$$\begin{aligned} L &= \sum_{j=1}^{n-1} \left| \frac{\partial \ell^{(i,n-1)}}{\partial z_j}(z_1, \dots, z_{n-1}) - \frac{\partial \ell^{(i,n)}}{\partial z_j}(z_1, \dots, z_n) \right| = \sum_{j=1}^{n-1} \left| \frac{e^{z_j}}{\sum_{k=1}^{n-1} z_k} - \frac{e^{z_j}}{\sum_{k=1}^n z_k} \right| \\ &= \sum_{j=1}^{n-1} \frac{e^{z_j}}{\sum_{k=1}^{n-1} z_k} - \frac{e^{z_j}}{\sum_{k=1}^n z_k} \end{aligned}$$

Where we removed the absolute value on the last term since all values are positive. We observe that the first term sums up to 1, and the last one corresponds to  $1 - \frac{e^{x_n}}{\sum_{k=1}^n e^{x_k}} = 1 - p_n$ , so we have that the above expression is given by

$$L = 1 - \left( \sum_{j=1}^{n-1} \frac{e^{z_j}}{\sum_{k=1}^n e^{z_k}} \right) = 1 - (1 - p_n) = p_n \quad (18)$$

$$(19)$$

Combining eq. (14), eq. (17), and eq. (18), we must have

$$\begin{aligned} G_1 + G_2 + (n-1)L &= 2(1 - p_n) + (n-1)p_n + (n-1)p_n \\ &= 2(1 + (n-2)p_n) \end{aligned}$$

Since the contrastive loss uses the cosine similarity, we have that the inputs  $(z_1, \dots, z_n)$  to  $\ell^{(i,n)}$ , given by terms of the form  $\mathbf{S}^n(x_i, \mathbf{x}')$ . This implies that  $|z_i| < 1$  for all  $i$ . Consequently, the last term is maximized when  $z_n = 1$  and  $z_k = -1$  for  $k \leq n-1$ , yielding

$$\begin{aligned} G_1 + G_2 + (n-1)L &\leq 2 \left( 1 + \frac{(n-2)e}{e + (n-1)e^{-1}} \right) \\ &= 2 \left( 1 + \frac{(n-2)e^2}{e^2 + (n-1)} \right) \end{aligned} \quad (20)$$

Where we multiplied by  $e$  the numerator and denominator on the last step. The result follows from theorem 4.2.  $\square$

## A.1 Proof of Lemma 4.6

**Lemma.** *lemma 4.6 Let  $\ell^{(i,n)}$  denote the spreadout regularizer of example 2. Then  $\ell^{(i,n)}$  satisfies the conditions of Theorem 4.2 for*

$$G_1 + G_2 + (n-1)L \leq 6$$

## B Experiment Details

This appendix gives more details about the numerical experiments in Section 5.

All models were trained on a single NVidia V100 GPU using a cloud computing platform with 64 GB of RAM.

### B.1 Pre-training on CIFAR10

#### Model Specification, Dataset Details, and Hyperparameters

For reproducibility, we now give the details of the model, the hyperparameters of the above variants, and the training setup.  $\Phi$  is a small embedding net model consisting of three 2D convolution layers followed by one embedding layer. The convolution layers used a 3-by-3 kernel with a stride of 2, a ReLU output activation function, a Kaiming-normal kernel initializer, and (sequentially) chose output channels of 8, 16, and 32, respectively. The embedding layer generated an output of dimension 8 and used a Xavier-normal initializer.

The learning rates for Logit-DP, Naive-DP, and Non-Private were  $10^{-2}$ ,  $10^{-2}$ , and  $10^{-3}$ . All variants used the standard Adam optimizer (iteration scheme) for training and used the canonical 80-20 train-test split of the CIFAR10 dataset. The batch size during training was 400 and the entire testing dataset was used for evaluating test metrics. Moreover, each variant was run for five epochs over the entire training dataset.

For the DP variants, we fixed the desired  $\ell_2$  sensitivity to be 1.0 and chose a noise multiplier so that  $\epsilon$ -DP was achieved for  $\epsilon = 5.0$ . All hyperparameter tuning was done through a grid search of various learning rates ( $10^{-4}$ ,  $10^{-3}$ ,  $10^{-2}$ ) and  $\ell_2$  sensitivities ( $10^{-2}$ ,  $10^{-1}$ ,  $10^0$ ).

#### Confusion Matrices and Absolute Test Metrics

|             | Accuracy | Top Recall | Top Precision | Top $F_\beta$ Score |
|-------------|----------|------------|---------------|---------------------|
| Logit-DP    | 0.199    | 0.304      | 0.298         | 0.299               |
| Naive-DP    | 0.151    | 0.217      | 0.218         | 0.218               |
| Non-Private | 0.268    | 0.378      | 0.379         | 0.378               |

Table 3: Aggregate CIFAR10 test metrics generated by the confusion matrix  $C$  at the last test point over ten runs. Accuracy is defined as  $\sum_i C_{ii} / \sum_{i,j} C_{ij}$ . The recall, precision, and  $F_\beta$  scores are the average of the best observed metric over all ten CIFAR10 classes.

### B.2 Fine-tuning on CIFAR10

#### Model Specification, Dataset Details, and Hyperparameters

For reproducibility, we now give the details of the model, the hyperparameters of the above variants, and the training setup.  $\Psi$  is a three-layer fully-connected neural network whose layer output dimensions are 64, 32, and 20 in sequence.

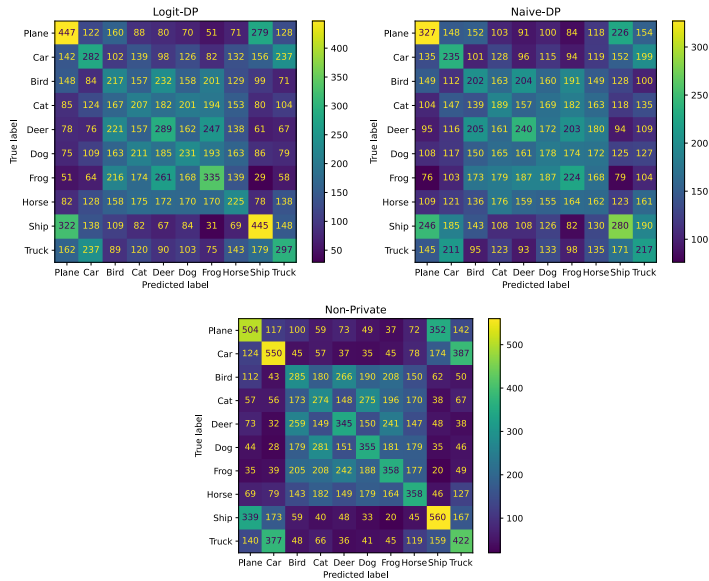


Figure 3: Averaged CIFAR10 confusion matrices at the last testing step. Values are rounded down to the nearest whole number.

The learning rate for all variants was  $10^{-2}$ . All variants used the standard Adam optimizer (iteration scheme) for training and used the canonical 80-20 train-test split of the CIFAR100 dataset. The batch size during training was 400 and the entire testing dataset was used for evaluating test metrics. Moreover, each variant was run for ten epochs over the entire training dataset.

For the DP variants, we fixed the desired  $\ell_2$  sensitivity to be 1.0 and chose a noise multiplier so that  $\epsilon$ -DP was achieved for  $\epsilon = 5.0$ . All hyperparameter tuning was done through a grid search of various learning rates ( $10^{-4}$ ,  $10^{-3}$ ,  $10^{-2}$ ) and  $\ell_2$  sensitivities ( $10^{-2}$ ,  $10^{-1}$ ,  $10^0$ ).

#### Absolute Test Metrics

|             | Accuracy | Top Recall | Top Precision | Top $F_\beta$ Score |
|-------------|----------|------------|---------------|---------------------|
| Logit-DP    | 0.170    | 0.358      | 0.287         | 0.316               |
| Naive-DP    | 0.143    | 0.442      | 0.245         | 0.303               |
| Non-Private | 0.198    | 0.444      | 0.505         | 0.451               |

Table 4: CIFAR100 test metrics generated by the confusion matrix  $C$  at the last test point over one run. Accuracy is defined as  $\sum_i C_{ii} / \sum_{i,j} C_{ij}$  while top recall, precision, and  $F_\beta$  scores are the best observed metric over all CIFAR100 classes.